Supporting Information

Comprehensive investigation on the reciprocity of structure and enhanced photocatalytic performence in finned-tube structured $BiOBr/TiO_2$ heterojunction†

Chao Xue,[a] Xin Xu,[b] Guidong Yang*[a] and Shujiang Ding*[b]

[a] Department of Chemical Engineering, School of Chemical Engineering and Technology, Xi'an Jiaotong University, Xi'an, 710049, China.

[b] Department of Applied Chemistry, School of Science, State Key Laboratory for Mechanical Behavior of Materials, Xi'an Jiaotong University, Xi'an, 710049, China.

Corresponding authors.

E-mail addresses: guidongyang@mail.xjtu.edu.cn (G. Yang), dingsj@mail.xjtu.edu.cn (S. Ding).

Experimental section

Materials

All the chemical reagents were analytical grade without further purification and purchased from Sinopharm Chemical Reagent Co., Ltd.

Synthesis of sulfonated polydivinylbenzene nanotubes (SPNTs)

The pristine bamboo-like highly crosslinked polydivinylbenzene nanotubes (PNTs) were fabricated on a large scale via the cationic polymerization which the reaction occurred in ultrasonic assisted treatment, and a large quantity of white precipitation were produced within minutes at room temperature.[1-3] The as-prepared sulfonated PNTs (SPNTs) were obtain by sulfonic functionalization which introducing the negative functional groups ($-HSO_3$) onto the surface of PNTs. Typically, 0.2 g of PNTs were immersed in 30 mL of concentrated sulfuric acid and the mixtures were stirring for 24 h at 40 °C. Subsequently, the slurry was diluted by a large amount of deionized water. And then, the yellow precipitate was filtered and washed with deionized water and ethanol to remove the residual

sulfuric acid, respectively.[4,5]

Synthesis of TiO_2@SPNT composite

100 mg of SPNTs were dispersed into 10 mL of anhydrous ethanol under sonication for 150 min. Then the suspension was put inside an ice-water bath under high speed magnetic stirring for 10 min. 1.5 mL of tetra-n-butyl titanate (TBOT) was rapidly added to the above mixture with continuous stirring for 2 h to allow a saturated adsorption of the positively charged titanium precursor ions on the surface of SPNTs due to the electrostatic interaction. Afterwards, the sulfonated gel matrix of polymeric nanotubes were collected by centrifugation (4000 rpm) and re-dispersed with 10 mL of anhydrous ethanol under the ultrasonic for seconds. 1 mL of water was introduced into the system dropwise and kept stirring at 0 °C for 2 h, subsequently. Finally, the as-obtained product was separated by centrifugation (4000 rpm) and dried at ambient temperature.

Synthesis of sulfonic functionalized one-dimensional (1D) TiO_2 nanotubes (TiO_2 NTs)

The white 1D TiO_2 nanotubes were obtained by calcinating TiO_2@SPNT composite nanocables at 450 °C for 2 h in air environment (heating rate: 1°C·min^{-1}) which removing the PNTs template and turning the amorphous TiO_2 into the anatase phase. To obtain the functionalized 1D TiO_2 nanotubes, the as-prepared 1D TiO_2 nanotubes (0.1 g) were ultrasonic dispersed into 10 mL of H_2SO_4 solution (1 M). After being stirred for 2 h at 60 °C, the precipitate was collected by centrifugation and washed with deionized water for several times. Subsequently, the as-prepared samples were dried at 110 °C for 6 h and annealed at 450 °C for 2 h in air environment (heating rate: 1°C·min^{-1}) to graft the negative functional groups (-SO_4) from the surface of TiO_2 NTs forming the chelating ligand structure.

Synthesis of 1D finned-tube structured TiO_2@BiOBr heterojunction (TBNTs)

1D TBNTs were fabricated by a new facile and efficient solvothermal method. Briefly, 0.3 mmoL of the as-synthesized functionalized 1D TiO_2 NTs, 0.2 g of PVP and 0.1 mmoL of $Bi(NO_3)_3 \cdot 5H_2O$ were dispersed into 10 mL of ethylene glycol (EG) solution by ultrasonication, respectively. After magnetic stirring for 2h, the slurry was transferred into a 50 mL of Teflon-lined stainless steel autoclave. 10 mL of EG solution consisting of cetyltrimethyl ammonium bromide (0.3 mmoL) were then added to the above mixture. After that, the white homogeneous suspension was subjected to solvothermal treatment in a 50 mL Teflon-lined autoclave at 160 °C for 30 min and then cooled to room temperature to prepare TBNTs. The resulting pale lemon yellow product was collected by centrifugation (4,000 rpm), washed with deionized water for several times and subsequently dried in a vacuum oven at 60 °C overnight. Also, two-dimensional (2D) pure BiOBr nanoplates aggregates were synthesized

according to the same method as mentioned above, except for the addition of the modified 1D TiO_2 NTs. For comparison, the mechanical mixture of TiO_2-BiOBr (MTB) was prepared by mechanical mixing method which mixing the synthesized lemon yellow 2D pure BiOBr nanoplates and the as-fabricated modified 1D TiO_2 nanotubes at the desired mole ratio. The content of each component mentioned above is according to the results of energy dispersive X-ray spectral semi-quantitative analysis from sample TBNTs-1 (Fig. S4a).

Materials characterization

The samples were characterized by different analytic techniques. In order to identify the phase composition, powder XRD patterns were recorded on an X-ray powder diffractometer with Cu Kα radiation (XRD; SHIMADZU, Lab X XRD-6000; λ=1.54056 Å) over a 2θ range of 20-80°. The Fourier transform infrared spectra (FT-IR) were measured on a Nicolet avatar 360 FT-IR spectrometer with KBr as the reference sample at room temperature. The surface morphologies and nanostructures of all samples were performed by scanning electron microscopy (FESEM; JEOL, JSM-6700F, 200 kV) and transmission electron microscopy (TEM; JEOL, JEM-2100). The component of as-prepared samples was also detected by energy dispersive X-ray spectrometry (EDX). STEM and EDX elemental mapping were acquired using energy-dispersive X-ray spectroscopy attached to JEM-2100F (TEM, JEOL). To investigate the optical properties, UV-Vis diffuse reflectance spectra (DRS) were measured on a Hitachi UV-4100 instrument employed with a lab-sphere diffuse reflectance accessory. The concentration of the contaminant was evaluated by a UV-Vis spectrophotometer (UV1900PPC, Yayan Electronic Science and Technology Institute Co. Ltd., Shanghai, China). The photoluminescence (PL) emission spectra of the as-synthesized samples were recorded at room temperature on a HORIBAJY Fluorolog-3 type fluorescence spectrophotometer with an excitation wavelength of 325 nm.

Photoelectrochemical measurements

All photoelectrochemical tests were performed by using a CHI 760D (Shanghai Chenhua Ltd., China) electrochemical workstation with a standard three-electrode cell system with platinum wire electrode as a counter electrode, the as-prepared photocatalyst electrode as a working electrode, and Ag/AgCl (saturated KCl) electrode as a reference electrode under ambient temperature (25℃). Typically, the working electrodes were prepared as follows: 3 mg of as-prepared photocatalyst was added into the mixed solution of ultrapure water (2 mL), isopropanol (0.5 mL) and perfluorosulfonic acid polymer (Nafion, 0.05 mL), then 0.03 mL of the obtained slurry was coated onto the surface of the cleaned platinized carbon electrode (effective diameter of 3 mm) and dried at room temperature

overnight to form uniform film electrodes. The transient photocurrent response was performed on the electrochemical analyzer by a 300 W xenon lamp (≥420 nm), positioned 10 cm far from the surface of the working electrode, as a light source. An electrolyte solution with a concentration of 2 M Na_2SO_4 aqueous solution (100 mL) was used in a quartz cell. Bias voltage was 0.50 V (Vs. SCE). The electrochemical impedance spectra (EIS) were performed in the frequency range of 1 Hz-100 kHz (AC voltage of 5 mV amplitude). And 0.2 M KCl and 0.005 M $K_3[Fe(CN)_6]$ in a 1:1 (v:v) mixture served as the detecting electrolyte.

Photocatalytic activity measurements

The photocatalytic activity of 1D finned-tube structured TiO_2@BiOBr heterojunction has been evaluated by using the Rhodamine B (RhB) solution of 10mg/L as the degradation object under visible-light irradiation at ambient temperature. A 300 W of Xenon lamp (Nbet, HSX-F/UV300, Beijing, China) was furnished as visible light source which equipped with a 420 nm ultraviolet cut-off glass filter to remove UV light. In a typical reaction, the mixture containing 0.07 g of the photocatalyst and 70 mL of RhB solution was dispersed in a photocatalytic reactor with circulating water cooling system. Subsequently, the suspension was continuously stirred in the dark for 40 min to ensure that the mixed solution reached adsorption-desorption equilibrium. During the photoreaction, 3 mL of suspension was removed from the reactor at intervals of 3 min and then centrifuged. The concentration of the supernatant was further evaluated by a UV-vis spectrophotometer, subsequently.

Recycling experiments test

The operation of recycling experiments for photodegradation of RhB solution by as-prepared samples is the same with that of photocatalytic activity measurements, the only difference is that after visible light illuminating for 24 min in each cycle, 3 mL of suspension was removed from the reactor and then centrifuged for further analysis. In order to recycle the photocatalyst, the rest of the solution was centrifuged, dried at 60 °C for 1h in an oven and weighted. During the next run recycling experiment, the photocatalyst mentioned above was dispersed in a photocatalytic reactor containing corresponding amount of fresh RhB solution. In the whole recycling experiments, we needed to do seven photocatalytic activity tests, totally.

Active species trapping experiments

To further determine the main reactive radical species involved in the photocatalytic process, the radicals and holes trapping experiments were designed by adding various scavengers to the TBNTs-1 sample. In the present work, different scavenges of ethylenediaminetetraacetic acid disodium (EDTA-2Na), isopropyl alcohol (IPA; 1

mM) and benzoquinone (BQ; 10 mM) were used as scavenge the holes (h^+), hydroxyl radicals (·OH), and superoxide radical anions ($\cdot O_2^-$) species in the photodegradation of RhB, respectively. The trapping experiment was conducted similarly to that of the photocatalytic degradation of RhB procedures except that different doses of the scavenger were introduced separately into the RhB solutions prior to the addition of the photocatalyst.

Figures

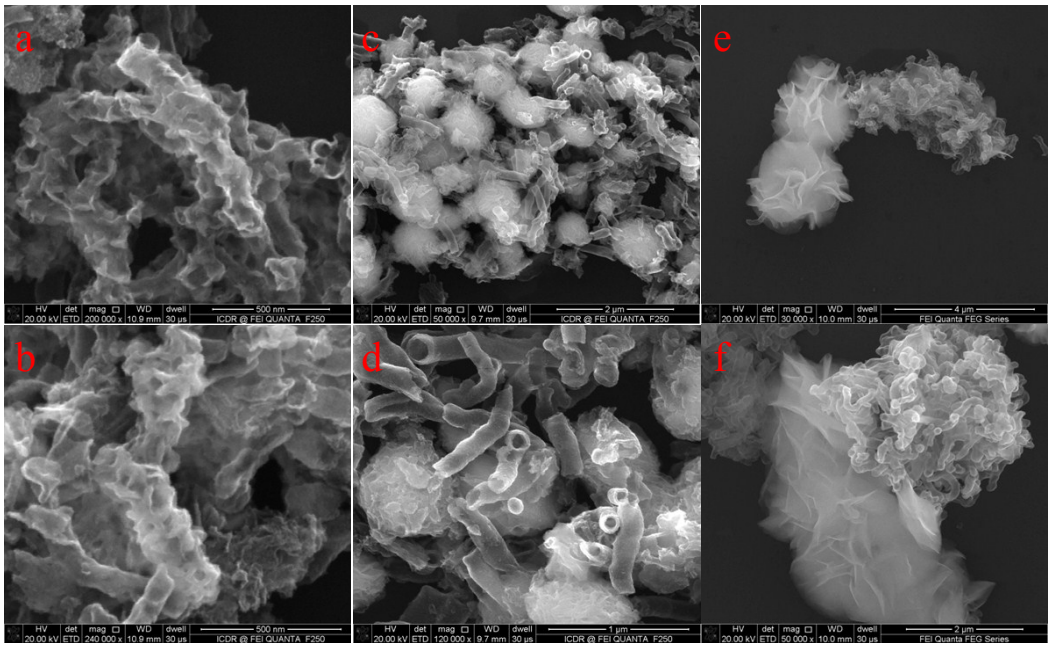

Figure S1. SEM images of the finned-tube structured TiO_2@BiOBr heterojunctions fabricated with different solvothermal times. (a-b) TBNTs-2 sample: 45 min, (c-d) TBNTs-3 sample: 60 min, and (e-f) TBNTs-4 sample: 120 min.

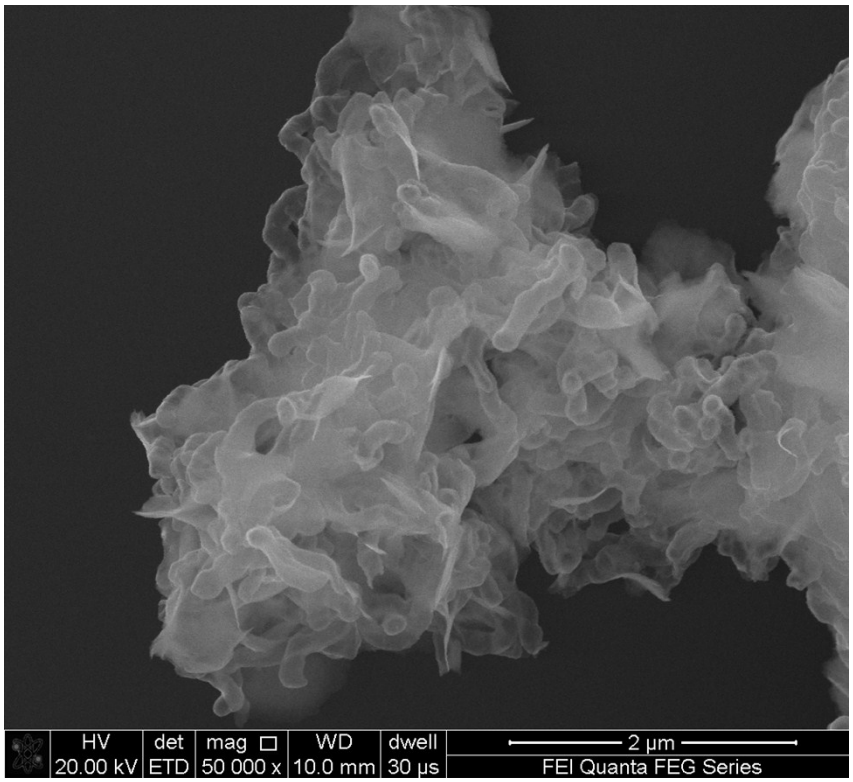

挨着

Figure S2. SEM image of 1D finned-tube structured TiO_2@BiOBr heterojunctions without PVP surfactant during the solvothermal synthesis (TBNTs-5 sample).

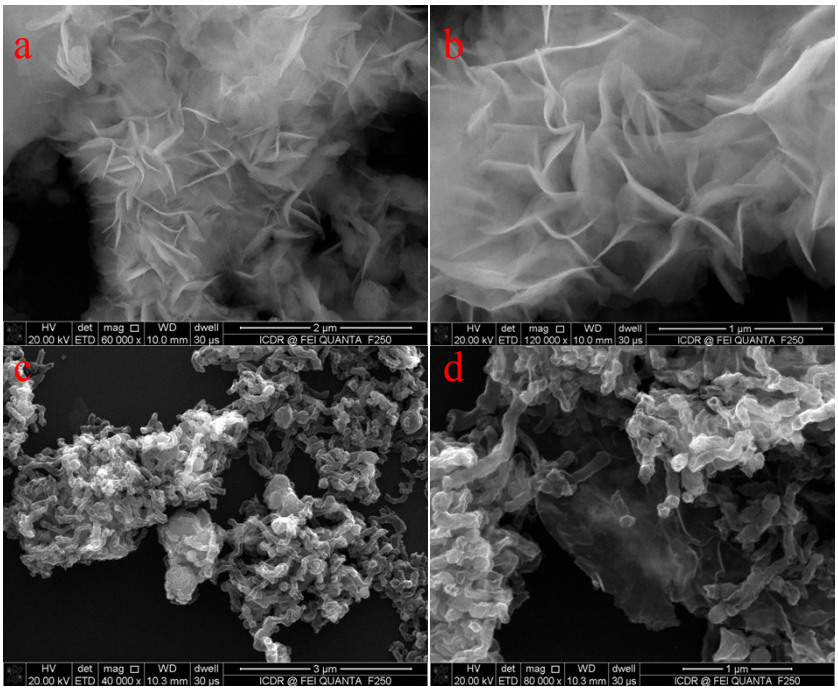

Figure S3. SEM images of samples. (a-b) pure BiOBr nanoplates and (c-d) MTB.

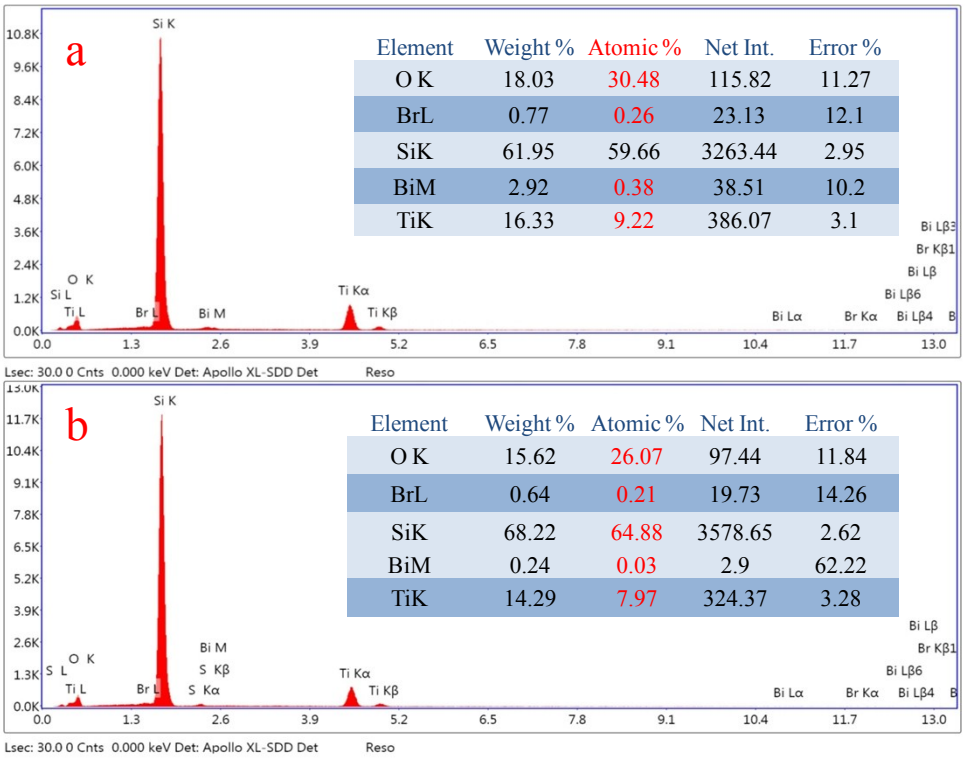

Figure S4. EDX spectrum of samples. (a) TBNTs-1 and (b) MTB.

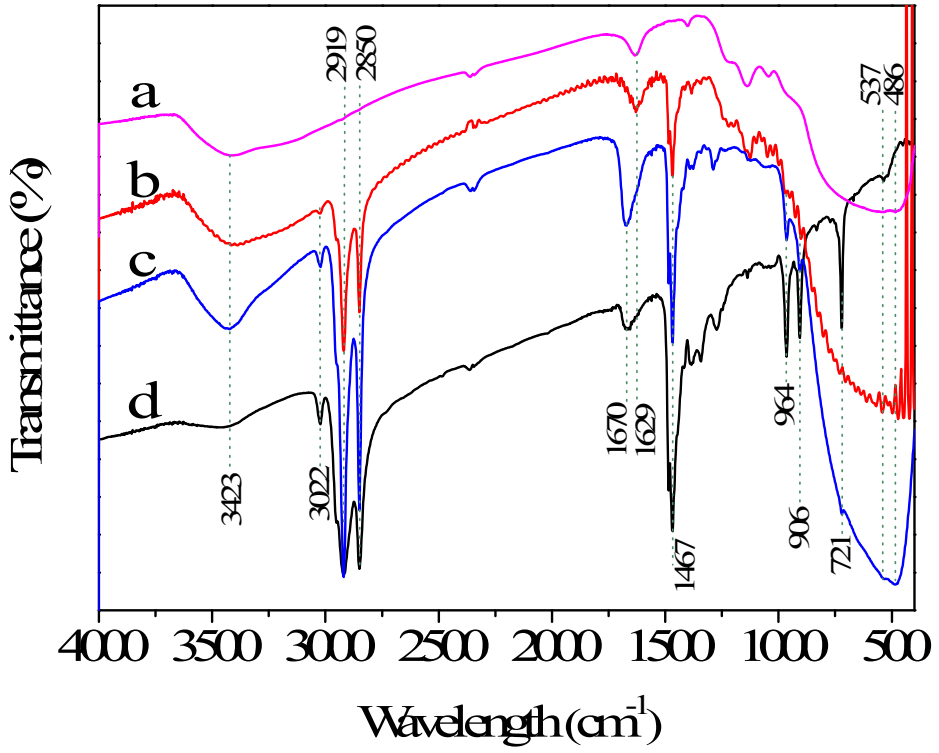

Figure S5. Fourier transform infrared (FT-IR) spectra of samples. (a) Sulfated TiO_2 NTs; (b) MTB; (c) TBNTs-1, and (d) Pure BiOBr nanoplates.

The broad adsorption band centered at 3423 cm^{-1} and the absorption peaks in the range of 1629-1670 cm^{-1} can be ascribed to the stretching and bending vibrations of hydroxyl groups (-OH) associating with absorbed H_2O molecules, respectively.[6-8] For samples containing BiOBr, the characteristic peaks at 2850, 2919 and 3022 cm^{-1} are assigned to typical alkyl C-H stretching vibrations, while the strong peak observed at 1467 cm^{-1} corresponding to C-H in-plane bending vibrations of methylene.[9] It could also be clearly seen that the peaks present at 906 and 964 cm^{-1} are due to C-H out-of-plane bending vibrations of residual EG, PVP or CTAB. And these common functional groups will not affect the photocatalytic performance of the as-prepared photocatalyst. Further observation shows that the as-prepared TBNTs-1 sample exhibits a significant decrease for two adsorption bands at 537 and 721 cm^{-1} corresponding to the Bi-O stretching mode compared with pure BiOBr nanoplates.[10-13] Furthermore, for samples containing TiO_2, the broad absorption band existed at 400-800 cm^{-1} region represents the typical Ti-O stretching and Ti-O-Ti bridging stretching modes.[14-15] The result of FT-IR spectra analysis is consistent with that of the EDX analysis.

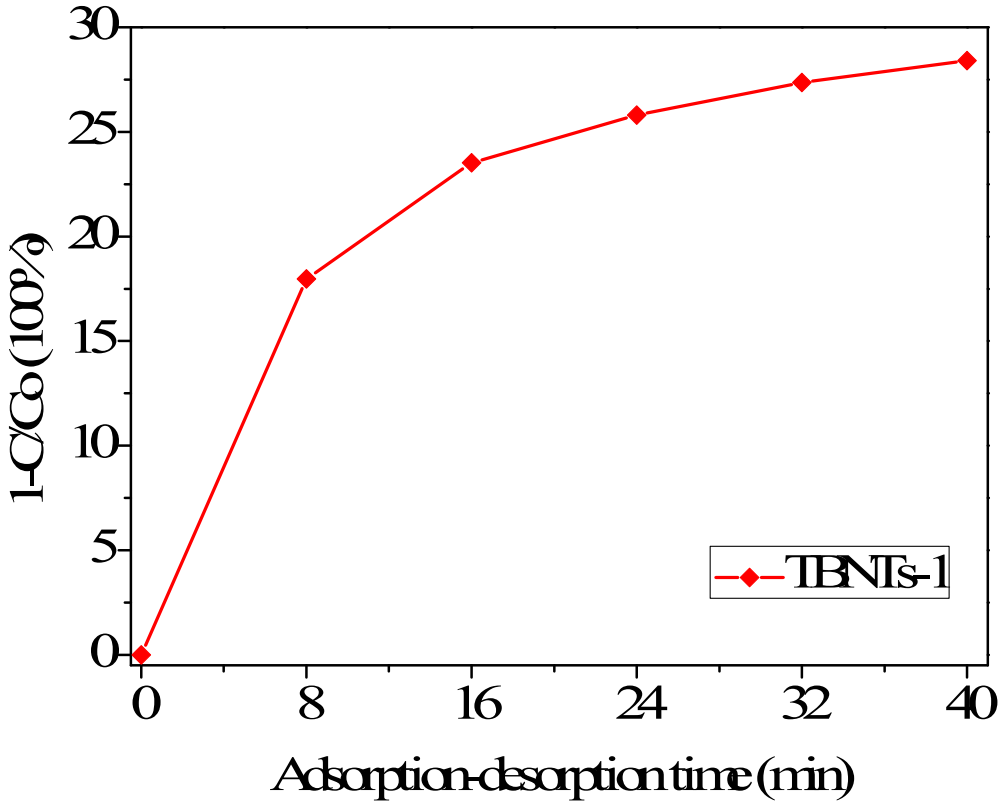

Figure S6. Plots of the adsorption capacity of RhB versus adsorption-desorption time by TBNTs-1 sample.

The Kubelka-Munk formula:

$$\alpha h\nu = A(h\nu - Eg)^{n/2} \quad (1)$$

where α, h, ν, Eg and A are the absorption coefficient, Planck constant, light frequency, band gap energy and a constant, respectively.[9,10,16,17] n is determined by characteristics of transition in the semiconductor (n=1 for direct transition and n = 4 for indirect transition). The values of n for BiOBr and anatase TiO_2 sample are taken as 4.[18,19] Therefore, the band gaps of all samples were estimated from the extrapolated intercept of the plot $(\alpha h\nu)^{1/2}$ versus photo energy (hν).

The atom's Mulliken electronegativity equation:

$$E_{VB} = \chi - E_c + \frac{1}{2}E_g \quad (2)$$

where E_{VB} is the VB edge potential, χ is the absolute electronegativity of the semiconductor (6.17 eV for BiOBr), which is the geometric mean of the electronegativity of the constituent atoms, Ec is the energy of free electrons on hydrogen scale (about 4.5 eV), Eg is the band gap energy of the semiconductor, respectively.[17,20-22]

References

1 W. Ni, F. Liang, J. Liu, X. Qu, C. Zhang, J. Li and Q. Wang, Z. Yang, *Chem. Commun.*, 2011, **47**, 4727-4729.

2 Y. Tang, L. Liu, X. Wang, H. Zhou and D. Jia, *RSC Adv.*, 2014, **4**, 44852-44857.

3 H. Zhou, L. Liu, X. Wang, F. Liang, S. Bao, D. Lv, Y. Tang and D. Jia, *J. Mater. Chem. A*, 2013, **1**, 8525-8528.

4 X. Xu, H. Tan, K. Xi, S. Ding, D. Yu, S. Cheng, G. Yang, X. Peng, A. Fakeeh and R. V. Kumar, *Carbon*, 2015, **84**, 491-499.

5 X. Xu, G. Yang, J. Liang, S. Ding, C. Tang, H. Yang, W. Yan, G. Yang and D. Yu, *J. Mater. Chem. A*, 2014, **2**, 116-122.

6 J. Fu, Y. Tian, B. Chang, F. Xi and X. Dong, *J. Mater. Chem.*, 2012, **22**, 21159-21166.

7 R. Yuan, T. Chen, E. Fei, J. Lin, Z. Ding, J. Long, Z. Zhang, X. Fu, P. Liu, L. Wu and X. Wang, *ACS Catal.*, 2011, **1**, 200-206.

8 Y. Tian, B. Chang, J. Lu, J. Fu, F. Xi and X. Dong, *ACS Appl. Mater. Interfaces*, 2013, **5**, 7079-7085.

9 A. Dash, S. Sarkar, V. N. Adusumalli and V. Mahalingam, *Langmuir*, 2014, **30**, 1401-1409.

10 F. Chang, Y. Xie, J. Zhang, J. Chen, C. Li, J. Wang, J. Luo, B. Deng and X. Hu, *RSC Adv.*, 2014, **4**, 28519-28528.

11 C. Xu, H. Wu and F. L. Gu, *J. Hazard. Mater.*, 2014, **275**, 185-192.

12 Z. Liu, B. Wu, Y. Zhu, D. Yin and L. Wang, *Catal. Lett.*, 2012, **142**, 1489-1497.

13 X. X. Wei, C. M. Chen, S. Q. Guo, F. Guo, X. M. Li, X. X. Wang, H. T. Cui, L. F. Zhao and W. Li, *J. Mater. Chem. A*, 2014, **2**,

4667-4675.

14 C. Xue, T. Wang, G. Yang, B. Yang and S. Ding, *J. Mater. Chem. A*, 2014, **2**, 7674-7679.

15 G. Yang, B. Yang, T. Xiao and Z. Yan, *Appl. Surf. Sci.*, 2013, **283**, 402-410.

16 Y. R. Jiang, H. P. Lin, W. H. Chung, Y. M. Dai, W. Y. Lin and C. C. Chen, *J. Hazard. Mater.*, 2015, **283**, 787-805.

17 L. Ye, Y. Su, X. Jin, H. Xie and C. Zhang, *Environ. Sci.: Nano*, 2014, **1**, 90-112.

18 J. Chen, M. Guan, W. Cai, J. Guo, C. Xiao and G. Zhang, *Phys. Chem. Chem. Phys.*, 2014, **16**, 20909-20914.

19 K. Li, H. Zhang, Y. Tang, D. Ying, Y. Xu, Y. Wang and J. Jia, *Appl. Catal., B: Environ*, 2015, **164**, 82-91.

20 W. Zhang, Q. Zhang and F. Dong, *Ind. Eng. Chem. Res.*, 2013, **52**, 6740-6746.

21 J. Di, J. Xia, Y. Ge, L. Xu, H. Xu, J. Chen, M. He and H. Li, *Dalton Trans.*, 2014, **43**, 15429-15438.

22 H. Lin, J. Cao, B. Luo, B. Xu and S. Chen, *Chin. Sci. Bull.*, 2012, **57**, 2901-2907.